Comparing the Normalized Difference Infrared Index (NDII) with root zone storage in a lumped conceptual model

N. Sriwongsitanon[1], H. Gao[2], H. H. G. Savenije[2], E. Maekan[1], S. Saengsawang[1], S. Thianpopirug[1]

[1]{Department of Water Resources Engineering, Faculty of Engineering, Kasetsart University}

[2]{Water Resources Section, Delft University of Technology, Delft, the Netherlands}

Correspondence to: H.H.G. Savenije (h.h.g.savenije@tudelft.nl)

Abstract

With remote sensing we can readily observe the Earth's surface, but direct observation of the sub-surface remains a challenge. In hydrology, but also in related disciplines such as agricultural and atmospheric sciences, knowledge on the dynamics of soil moisture in the root zone of vegetation is essential, as this part of the vadose zone is the core component controlling the partitioning of water into evaporative fluxes, drainage, recharge and runoff. In this paper we compared the catchment-scale soil moisture content in the root zone of vegetation, computed by a lumped conceptual model, with the remotely sensed Normalised Difference Infrared Index (NDII) in the Upper Ping River Basin (UPRB) in Northern Thailand. The NDII is widely used to monitor the Equivalent Water Thickness (EWT) of leaves and canopy. Satellite data from the Moderate Resolution Imaging Spectro-radiometer (MODIS) were used to determine the NDII over an 8-day period, covering the study area from 2001 to 2013. The results show that NDII values decrease sharply at the end of the wet season in October and reach lowest values near the end of the dry season in March. The values then increase abruptly after rains have started, but vary in an insignificant manner from the middle to the late rainy season. This paper investigates if the NDII can be used as a proxy for moisture deficit and hence for the amount of moisture stored in the root zone of vegetation, which is a crucial component of hydrological models. During periods of moisture stress, the 8-day average NDII values were found to correlate well with the 8-day average soil moisture content (S_u) simulated by the lumped conceptual hydrological rainfall-runoff model FLEX for 8 sub-catchments in the Upper Ping basin. Even the deseasonalized S_u and NDII (after subtracting the dominant seasonal signal) showed good correlation during periods of moisture stress. The results illustrate the potential of the NDII as a proxy for catchment-scale root zone moisture deficit and as a potentially valuable constraint for the internal dynamics of hydrological models. In dry periods, when plants are exposed to water stress, the EWT (reflecting leaf-water

deficit) decreases steadily, as moisture stress in the leaves is connected to moisture deficits in the root zone. When subsequently the soil moisture is replenished as a result of rainfall, the EWT increases without delay. Once leaf-water is close to saturation - mostly during the heart of the wet season - leaf characteristics and NDII values are not well correlated. However, for both hydrological modelling and water management the stress periods are most important, which is why this product has the potential to becoming a highly efficient model constraint, particularly in ungauged basins.

1. Introduction

Estimating the moisture content of the soil from remote sensing is one of the major challenges in the field of hydrology (e.g. De Jeu et al., 2008; Entekhabi et al., 2010). Soil moisture is generally seen as the key hydrological state variable determining the partitioning of fluxes (into direct runoff, recharge and evaporation) (Liang et. al., 1994), the interaction with the atmosphere (Legates et. al., 2011), and the carbon cycle (Porporato et al., 2004). The root zone of ecosystems, being the dynamic part of the unsaturated zone, is the key part of the soil related to numerous sub-surface processes (Shukla and Mintz, 1982). Several remote sensing products have been developed especially for monitoring soil moisture (e.g. SMOS, ERS and AMSR-E), but until now correlations between remote sensing products and observed soil moisture at different depths have been modest at best (Parajka et al., 2006; Ford et al., 1997). There are a few possible explanations. One is that it is not (yet) possible to look into the soil deep enough to observe soil moisture in the root zone of vegetation (Shi et al., 1997; Entekhabi et al., 2010), second is that soil moisture observations at certain depths are maybe not the right indicators for the amount of moisture stored in the root zone (Mahmood and Hubbard, 2007), which is rather determined by the vegetation dependent, spatially variable three-dimensional distribution and density of roots.

These mainstream methods to derive soil moisture from remote sensing have concentrated on direct observation of soil moisture below the surface. The vegetation, through the Vegetation Water Content (VWC), perturbs this picture. As a result, previous studies have tried to determine the VWC from a linear relationship with the Equivalent Water Thickness (EWT) that is measured by the Normalised Difference Infrared Index (NDII) (e.g. Yilmaz et al., 2008). The NDII was developed by Hardisky et al. (1983) using ratios of different values of near infrared reflectance (NIR) and short wave infrared reflectance (SWIR), defined by: $(\rho_{NIR}-\rho_{SWIR})/(\rho_{NIR}+\rho_{SWIR})$, similar to the NDVI, which is defined by discrete red and near infrared. Besides for determining the water content of vegetation, the NDII can be effectively used to detect plant water stress according to the property of shortwave infrared reflectance, which is negatively related to leaf water content due to the large absorption by the leaf (e.g. Steele-Dunne et al., 2012; Friesen et al., 2012; Van Emmerik et al., 2015). Many studies have found relationships between the equivalent water thickness (EWT) and reflectance at the near-infrared (NIR) and shortwave infrared (SWIR) portion of the spectrum used for deriving NDII (Hardisky et al., 1983; Hunt and Rock, 1989; Gao, 1996; Ceccato et al., 2002; Fensholt and Sandholt, 2003). Yilmaz et al. (2008) found a significant linear relationship ($R^2 = 0.85$) between equivalent water thickness (EWT) and NDII. Subsequently, they tried to determine a relationship between EWT and vegetation water content (VWC), in order to be able to correct direct moisture observations from space. However, these relationships appeared to be vegetation and crop-type dependent.

Water is one of the determinant environmental variables for vegetation growth, especially in water-limited ecosystems during dry periods. From plant physiology point of view, water absorption from the root zone is driven by osmosis. Subsequently, water transport from the roots to the leaves is driven by water potential differences, caused by diffusion of water out of stomata, called transpiration. This physiological relationship supports the correlation between root zone soil moisture content, moisture tension in the leaves and the water content of plants.

Hence, the root zone moisture deficit is connected to the water content of the canopy/leaves, because soil moisture suction pressure and moisture content in the leaves are directly connected (Rutter and Sands, 1958). The NDII was developed to monitor leave water content (Hardisky et al., 1983), so one would expect a direct relation between NDII and root zone moisture deficit. The deficit again is a direct function of the amount of moisture stored in the root zone.

So if leaf water thickness and the suction pressure in the root zone are connected, then the NDII would directly reflect the moisture content of the root zone. It would only reflect the moisture content in the influence zone of roots and not beyond that. Hence the NDII could become a powerful indicator for monitoring root zone moisture content, providing an integrated, depth-independent estimation of how much water is accessible to roots, available for vegetation. In other words, the NDII would allow us to see vegetation as a sort of natural manometer, providing us with information on how much water is available in the sub-surface for use by vegetation. It would be an integrated indicator of soil moisture in the root zone, available directly at the scale of interest.

Thus, the hypothesis is that we can monitor the moisture content in the root zone from the observed moisture state of the vegetation by means of the NDII.

In this paper, we tested whether there exists a direct and functional relationship between a remote sensing product (the NDII) and the amount of moisture stored in the root zone, as simulated by a semi-distributed conceptual hydrological model, in which the root zone moisture content is a key state variable in the short and long term dynamics of the rainfall-runoff signal. Because the NDII is an indicator for water stress, the index is only expected to show a strong link with the moisture content of the root zone when there is a soil moisture deficit. Without water stress occurring within the leaves, particularly during wet periods, NDII would possibly not reflect variation in root zone soil moisture content (Korres et al., 2015).

The analysis was done using data from eight sub-basins of the Upper Ping River Basin (UPRB), a tropical seasonal evergreen catchment in northern Thailand. This catchment is adequate for the purpose because it has eight well-gauged sub-basins with clearly different aridity characteristics and strong seasonality, providing a good testing ground for the comparison.

The remotely sensed NDII values have been compared to the root zone storage as modelled by a semi-distributed conceptual model; semi-distributed meaning that for each sub-catchment a separate conceptual model has been used. The different sub-catchments demonstrate a variety of climatic properties that allow a more rigorous test than a fully lumped model could provide. In this way, a compromise has been found between the complexity and data requirements of a fully distributed model and the simplicity of a completely lumped model. One could argue that a fully distributed conceptual model would have been a better tool to assess the spatial and temporal pattern obtained by the NDII. This is correct, but this would have required the availability of more detailed spatially distributed forcing data (particularly rainfall), which was not available. Moreover, if a semi-distributed lumped model, potentially less accurate than a distributed model, provides a good correlation with NDVI, then this would be a tougher text than with a fully distributed model.

2. Study site and data

2.1 Study site

The Upper Ping River Basin (UPRB) is situated between latitude 17°14′30″ to 19°47′52″ N, and longitude 98°4′30″to 99°22′30″ E in Northern Thailand and can be separated into 14 sub-basins (Fig. 1) (Mapiam, et al., 2014). It has an area of approximately 25,370 km^2 in the provinces of Chiang Mai and Lam Phun. The basin landform ranges from an undulating to a rolling terrain with steep hills at elevations of 1,500 to 2,000 m, and valleys of 330 to 500 m (Mapiam and

Sriwongsitanon, 2009; Sriwongsitanon, 2010). The Ping River originates in Chiang Dao district, north of Chiang Mai, and flows downstream to the south to become the inflow for the Bhumiphol dam - a large dam with an active storage capacity of about 9.7 billion m^3 (Sriwongsitanon, 2010). The climate of the region is controlled by tropical monsoons, with distinctive dry and wet seasons and free from snow and ice. The rainy season is influenced by the southwest monsoon and brings about mild to heavy rainfall between May and October. Annual average rainfall and runoff of the UPRB are approximately 1,170 and 270 mm/y, respectively. Avoiding the influence of other factors, these catchments are ideal cases to concentrate on the relationship between NDII and root zone moisture content. The land cover of the UPRB is dominated by forest (Sriwongsitanon and Taesombat, 2011).

2.2 Data Collection

2.2.1 Rainfall data

Data from 65 non-automatic rain-gauge stations covering the period from 2001 to 2013 were used. 42 stations are located within the UPRB while 23 stations are situated in its surroundings. These rain gauges are owned and operated by the Thai Meteorological Department and the Royal Irrigation Department. Quality control of the rainfall data was performed by comparing them to adjacent rainfall data. For each sub-basin, daily spatially averaged rainfall, by inverse distance squared, has been used as the forcing data of the hydrological model.

2.2.2 Runoff data

Daily runoff data from 1995 to 2011 at 8 stations located in the UPRB were adequate to be used for FLEX calibration. These 8 stations are operated by the Royal Irrigation Department in Thailand. The locations of these 8 stations and the associated sub-basins are shown in Fig. 1. These 8 stations control the runoff of the eight sub-basins on which the eight lumped conceptual models were calibrated. Runoff data at these stations are not affected by large reservoirs and have been checked for their reliability by comparing them with rainfall data covering their catchment areas at the same periods. Catchment characteristics and available data periods for model calibration of the selected 8 sub-basins are summarized in Table 1.

2.2.3 NDII data

The satellite data used for calculating the NDII is the MODIS level 3 surface reflectance product (MOD09A1), which is available at 500 m resolution in an 8-day composite of the gridded level 2 surface reflectance products. Each product pixel contains the best possible L2G observation during an 8-day period selected on the basis of high observation coverage, low view angle, absence of clouds or cloud shadow, and aerosol loading. MOD09 (MODIS Surface Reflectance) is a seven-band product, which provides an estimate of the surface spectral reflectance for each band as it would have been measured at ground level without atmospheric scattering or absorption. This product has been corrected for the effects of atmospheric gases and aerosols (Vermote et al., 2011). The available MODIS data covering the UPRB from 2001 to 2013 were downloaded from ftp://e4ftl01.cr.usgs.gov/MOLT. The HDF-EOS Conversion Tool was applied to extract the desired bands (bands 2 (0.841-0.876 μm) and 6 (1.628-1.652 μm)) and re-projected into Universal Transverse Mercator (Zone 47N, WGS84) from the original ISIN mapping grid.

3. Methods

3.1 Estimating vegetation water content using near infrared and short wave infrared

Estimates of vegetation water content (the amount of water in stems and leaves) are of interest to assess the vegetation water status in agriculture and forestry and have been used for drought assessment (Cheng et al., 2006; Gao, 1996; Gao and Goetz, 1995; Ustin et al., 2004; Peñuelas et al., 1993). Evidence from physically-based radiative transfer models and laboratory studies suggests that changes in water content in plant tissues have a large effect on the leaf reflectance in several regions of the 0.7-2.5 μm spectrum (Fensholt and Sandholt, 2003). Tucker (1980) suggested that the spectral interval between 1.55 and 1.75 μm (SWIR) is the most suitable region for remotely sensed leaf water content. It is well known that these wavelengths are negatively related to leaf water content due to a large absorption by leaf water (Tucker, 1980; Ceccato et al., 2002). However, variations in leaf internal structure and leaf dry matter content also influence the SWIR reflectance. Therefore, SWIR reflectance values alone are not suitable for retrieving vegetation water content. To improve the accuracy in estimating the vegetation water content, a combination of SWIR and NIR (0.7 to 0.9 μm) reflectance information was utilized because NIR is only affected by leaf internal structure and leaf dry matter content but not by water content. A combination of SWIR and NIR reflectance information can remove the effect of leaf internal structure and leaf dry matter content and can improve the accuracy in retrieving the vegetation water content (Ceccato et al., 2001; Yilmaz et al., 2008; Fensholt and Sandholt, 2003).

On the basis of this idea, Hardisky et al. (1983) derived the NDII:

$$NDII = \frac{\rho_{0.85} - \rho_{1.65}}{\rho_{0.85} + \rho_{1.65}} \qquad (1)$$

where $\rho_{0.85}$ and $\rho_{1.65}$ are the reflectances at 0.85 μm and 1.65 μm wavelengths, respectively. NDII is a normalized index and the values theoretically vary between -1 and 1. A low NDII value and especially below zero means that reflectance from $\rho_{0.85}$ is lower than the reflectance from $\rho_{1.65}$ which indicates canopy water stress.

The 8-day NDII values, as collected from MODIS, were averaged over each sub-basin to allow comparison to the 8-day average S_u (root zone storage) values extracted from the FLEX model results at each of the 8 runoff stations.

We did not use field observations of soil moisture. One could argue that field observations should be used to link NDII to moisture stress. However, besides not being available, it is doubtful if point observations at fixed depth would provide a correct measure for the moisture content in the root zone. It is more likely that vegetation distributes its roots and adjusts its root density to the specific local conditions and that the root density and distribution is not homogeneous in space and depth.

3.2 The semi-distributed FLEX Model

FLEX (Fig. 2) is a conceptual hydrological model with an HBV-like model structure developed in a flexible modelling framework (Fenicia et al., 2011; Gao et al., 2014a; Gao et al., 2014b). The model structure comprises four conceptual reservoirs: the interception reservoir S_i (mm), the root zone reservoir representing the moisture storage in the root zone S_u (mm), the fast response reservoir S_f (mm), and the slow response reservoir S_s (mm). It also includes two lag functions representing the lag time from storm to peak flow (T_{lagF}), and the lag time of recharge from the root zone to the groundwater (T_{lagS}). Besides a water balance equation, each reservoir has process equations that connect the fluxes entering or leaving the storage compartment to the storage in the reservoirs (so-called constitutive functions). Table 2 shows the 15 equations of the FLEX model, discussed below. The 11 model parameters with their distribution values are shown in Table 3, which have to be determined by model calibration. Forcing data include the elevation-corrected daily average rainfall (Gao et al., 2014a), daily average, minimum and maximum air temperature, and potential evaporation derived by Hargreaves equation (Hargreaves and Samani, 1985).

3.2.1 Interception reservoir

The interception reservoir uses the water balance equation, Eq. (2), presented in Table 2. The interception evaporation E_{i} (mm d^{-1}) is calculated by potential evaporation E_0 (mm d^{-1}) and the storage of the interception reservoir S_i (mm) (Eq. (3)). There is no effective rainfall P_e (mm d^{-1}) as long as the S_i is less than its storage capacity $S_{i,max}$ (mm) (Eq. (4)) (de Groen and Savenije, 2006).

3.2.2 Root zone reservoir

The moisture content in the root zone is simulated by a 'reservoir' (Eq. (5)), that partitions effective rainfall into infiltration, and runoff R (mm d^{-1}), and determines the transpiration by vegetation E_t (mm d^{-1}). Being the key partitioning point, the root zone storage reservoir is the core of the FLEX model. For the partitioning between infiltration and runoff we applied the widely used beta function (Eq. (6)) of the Xinanjiang model (Zhao, 1992; Liang et al., 1992), developed based on the variable contribution area theory (Hewlett and Hibbert, 1967; Beven, 1979), but which can equally reflect the spatial probability distribution of runoff thresholds. The moisture storage in the root zone 'reservoir' is represented by S_u (mm). The beta function defines the runoff percentage C_r (-) for each time step as a function of the relative soil moisture content ($S_u/S_{u,max}$). In Eq. (6), $S_{u,max}$ (mm) is the root zone storage capacity, and β (-) is the shape parameter describing the spatial distribution of the root zone storage capacity over the catchment. In Eq. (7), the relative soil moisture and potential evaporation are used to determine the transpiration E_t (mm d^{-1}); C_e (-) indicates the fraction of $S_{u,max}$ above which the transpiration is no longer limited by soil moisture stress (E_t=E_0-E_i).

3.2.3 Response routine

In Eq. (8), R_f (mm d^{-1}) indicates the flow into the fast response routine; D (-) is a splitter to separate recharge from preferential flow. In Eq. (9), R_s (mm d^{-1}) indicates the flow into the groundwater reservoir. Equation (10) and (11) are used to describe the lag time between storm and peak flow. R_f (t-i+1) is the generated fast runoff from the root zone at time t-i+1; T_{lag} is a parameter which represents the time lag between storm and fast runoff generation; $c(i)$ is the weight of the flow in i-1 days before; and $R_{fl}(t)$ is the discharge into the fast response reservoir after convolution.

The linear response reservoirs, representing linear relationships between storages and releases, are applied to conceptualize the discharge from the fast runoff reservoir, and slow response reservoir. Eq. (12) presents the water balance of the fast reservoir, in which Q_{ff} (mm d^{-1}) is the direct surface runoff, with timescale K_{ff} (d), described by Eq. (13), activated when the storage of fast response reservoir exceeds the threshold $S_{f,max}$ (mm), and Q_f (mm d^{-1}) is the fast sub-surface flow, with time scale K_f (d), described by Eq. (14). The slow groundwater reservoir is described by Eq. (15), which generates the slow runoff Q_s (mm d^{-1}) with time scale K_s (d) described by Eq. (16). Q_m (mm

d^{-1}) is the total amount of runoff simulated from the three individual components, adding up: Q_{ff}, Q_f, and Q_s.

3.2.4 Model calibration

A multi-objective calibration strategy has been adopted in this study to allow for the model to effectively reproduce different aspects of the hydrological response, i.e. high flow, low flow and the flow duration curve. The model was therefore calibrated to three Kling-Gupta efficiencies (Gupta et al., 2009): 1) the K-G efficiency of flows (I_{KGE}) measures the performance of hydrograph reproduction especially for high flows; 2) the K-G efficiency of the logarithm of flows emphasizes low flows (I_{KGL}), and 3) the K-G efficiency of the flow duration curve (I_{KGF}) to represent the flow statistics.

The MOSCEM-UA (Multi-Objective Shuffled Complex Evolution Metropolis-University of Arizona) algorithm (Vrugt et al., 2003) was used as the calibration algorithm to find the Pareto-optimal solutions defined by the mentioned three objective functions. This algorithm requires 3 parameters including the maximum number of iterations, the number of complexes, and the number of random samples that is used to initialize each complex. To ensure fair comparison, the parameters of MOSCEM-UA were set based on the number of model parameters. Therefore, the number of complexes is equal to the number of free parameters n; the number of random samples is equal to $n*n*10$; and the number of iterations was set to 30000. The model is a widely validated model, which is only used here to derive the magnitude of the root zone moisture storage. Therefore validation is not considered necessary, since the model is merely meant to compare calibrated values of S_u with NDII.

3.3 Deseasonalization

Seasonal signals exist both in NDII and S_u time series. This can lead to spurious correlation. Therefore we deseasonalized both signals to eliminate this strong signal (Schaefli & Gupta, 2007) and subsequently compare the deviations from the seasonal signals of both NDII and S_u. Firstly, the NDII and S_u were normalized between 0 and 1. Then seasonal patterns of NDII and S_u were determined as the average seasonal signals, after which they were subtracted from the normalised data.

4. Results

4.1 Spatial and seasonal variation of NDII values over the UPRB

To demonstrate the spatial and seasonal behaviour of the NDII over the UPRB, the 8-day NDII values were aggregated to monthly values for 2001 to 2013. Figure 3 shows examples of monthly average NDII values for the UPRB in 2004, which is the year with the lowest annual average NDII value. The figure shows that NDII values are higher during the wet season (May to October) and lower during the dry season (from November to April). The lower amounts of rainfall between November and April cause a continuous reduction of NDII values. On the other hand, higher amounts of rainfall between May and October result in increasing NDII values. However, NDII values appear to vary little between July and October.

The average NDII values during the wet season, the dry season, and the whole year within the 13 years are presented in Table 4. The table also shows the order of the NDII values from the highest (number 1) to the lowest (number 13). It can be seen that the annual average NDII value for the whole basin is approximately 0.165, while the average values during the wet and dry season are about 0.211 and 0.118, respectively. The highest mean annual value (NDII = 0.177) occurred in 2002-2003 and the lowest (NDII = 0.149) in 2004-2005. The highest (NDII = 0.149) and lowest (NDII = 0.088) dry season values were reported in 2002-2003 and 2004-2005, respectively. On the other hand, the highest (NDII = 0.224) and lowest (NDII = 0.197) wet season values were observed in 2006-2007 and 2010-2011, respectively. It can be concluded that a dry season with relatively low moisture content and a wet season with high moisture content as specified by NDII values do not normally occur in the same year.

The 8-day NDII values were also computed for each of the 14 tributaries within the UPRB from 2001 to 2013. Table 5 shows the monthly averaged NDII values between 2001 and 2013 and the ranking order for each of the 14 tributaries. The results suggest that the Nam Mae Taeng, Nam Mae Rim, and Upper Mae Chaem, which have higher mean annual NDII values, have a higher moisture content than other tributaries; while Nam Mae Haad, Nam Mae Li, and Ping River Sections 2 are 3, with lower mean annual NDII values, have lower moisture content than other tributaries. Monthly average NDII values for these 6 tributaries are presented in Fig. 4. It can be seen that during the dry season, NDII values of the 3 tributaries with the lowest values are a lot lower than those of the 3 with the highest NDII values. However, NDII values for these 2 groups are not significantly different during the wet season. The figure also reveals that NDII values tend to continuously increase from relatively low values in March to higher values in June. The values slightly fluctuate during the wet season before sharply falling once again when the rainy season ends, and reach their minimum values in February.

4.2 FLEX Model results

Calibration of FLEX was done on the 8 sub-catchments that have runoff stations. The results are summarized in Table 6. The performance of the model was quite good as demonstrated in Table 7. In Fig. 5, the flow duration curves of runoff stations P.20 and P.21 are presented as examples of model performance. Table 7 shows the average Kling-Gupta efficiencies values for I_{KGE}, I_{KGL} and I_{KGF}, which indicate the performance of high flows, low flows, and flow duration curve for the 8 runoff stations. The results for the flow duration curve appear to be better than those of the high flows and especially the low flows. However, the overall results are acceptable and can be used for further analysis in this study.

4.3 Relation between NDII and root zone moisture storage (S_u)

The 8-day NDII values were compared to the 8 day average root zone moisture storage values of the FLEX model. It appears that during moisture stress periods, the relationship can be well described by an exponential function, for each of the 8 sub-catchments. Table 8 presents the coefficients of the exponential relationships as well as the coefficients of determination (R^2) for annual, wet season, and dry season values for each sub-catchment. The coefficients are merely meant for illustration. They should not be seen as functional relationships yet. The corresponding scatter plots are shown in Fig. 6. It can be clearly seen that the correlation is much better in the dry season than in the wet season. During the wet season, there may also be short period of moisture stress, where the exponential pattern can be recognized, but no clear relation is found when the vegetation does not experience any moisture stress.

Examples of deseasonalized and scaled time series of NDII and root zone storage (S_u) values for the sub-catchments P.20 and P.21 are presented in Figure 7. The scaled time series of the NDII and S_u values were calculated by dividing their value by the differences between their maximum and minimum values: $NDII/(NDII_{max}-NDII_{min})$ and $S_u/(S_{u,max}-S_{umin})$, respectively, while the maximum and the minimum are the values within the overall considered time series. Figure 7 shows that the scaled NDII and S_u values are highly correlated during the dry season, but less so during the wet season. These results confirm the potential of NDII to effectively reflect the vegetation water content, which, through the suction pressure exercised by the moisture deficit, relates to the moisture content in the root zone. During dry periods, or during dry spells in the rainy season, as soon as the leaves of the vegetation experience suction pressure, we see high values of the coefficient of determination.

If the soil moisture in the root zone is above a certain threshold value, then the leaves are not under stress. In the UPRB this situation occurs typically during the middle and late rainy season. The NDII then does not vary significantly while the root zone moisture storage may still vary, albeit above the threshold where moisture stress occurs. This causes a lower correlation between NDII and root zone storage during wet periods. Interestingly, even during the wet season dry spells can occur. We can see in Fig. 6, that during such a dry spell, the NDII and S_u again follow an exponential relationship.

We can see that the S_u, derived merely from precipitation and energy, is strongly correlated to the vegetation water observed by NDII during condition of moisture stress, without time lag (Figure 6, S1, S2). Introduction of a time lag resulted in reduction of the correlation coefficients (Supplementary material). This confirms the direct response of vegetation to soil moisture stress, which confirms that the NDII can be used as a proxy for root zone moisture content.

The deseasonalized results of dry periods in sub-catchments P.20 and P.21 are shown in Figure 7. We found these variations of deseasonalized NDII and S_u to be similar in these two sub-catchments, with the coefficients of determination (R^2) as 0.32 and 0.18 respectively in P.20 and P.21. More important than the coefficient of determination is the similarity between the deseasonalized patterns. For P.20, the year 2001 is almost identical, whereas the years 2004 and 2006 are dissimilar. In general the patterns are well reproduced, especially if we take into account the implicit uncertainties of the lumped hydrological model, the uncertainties in the 8-day derived NDII, and the data of precipitation and potential evaporation used in the model. The results of other tributaries can be found in the supplementary materials.

5. Discussion

5.1 Is vegetation a trouble-maker or a good indicator for the moisture content of the root zone?

In bare soil, remote sensors can only detect soil moisture until a few centimetres below the surface (~5cm) (Entekhabi et al., 2010). Unfortunately, for hydrological modelling, the moisture state of the bare surface is of only limited interest. What is of key interest for understanding the dynamics of hydrological systems is the variability of the moisture content of the root zone, in which the main dynamics take place. This variability determines the rainfall-runoff behaviour, the transpiration of vegetation, and the partitioning between different hydrological fluxes. However, observing the soil moisture content in the root zone is still a major challenge (Entekhabi et al., 2010).

What is normally done, is to link the moisture content of the surface layer to the total amount of moisture in the root zone. Knowing the surface soil moisture, the root zone soil moisture can be estimated by an exponential decay filter (Albergel et al., 2008; Ford et al., 2014) or by models (Reichle, 2008) However, the surface soil moisture is only weakly related with root zone soil moisture (Mahmood and Hubbard, 2007); it only works if there is connectivity between the surface and deeper layers and when a certain state of equilibrium has been reached (when the short term dynamics after a rainfall event has levelled out). It is also observed that the presence of vegetation prevents the observation of soil moisture and further deteriorates the results (Jackson and Schmugge, 1991). Avoiding the influence of vegetation in observing soil moisture (e.g. by SMOS or SMAP) is seen as a challenge by some in the remote sensing community (Kerr et al., 2001; Entekhabi et al., 2010). Several algorithms have been proposed to filter out the vegetation impact (Jackson and Schmugge, 1991), also based on NDII (e.g. Yilmaz et al., 2008). But is vegetation a trouble-maker, or does it offer an excellent opportunity to directly gauge the state of the soil moisture?

In this study, we found that vegetation rather than a problem could become key to sensing the storage dynamics of moisture in the root zone. The water content in the leaves is connected to the suction pressure in the root zone (Rutter and Sands, 1958). If the suction pressure is above a certain threshold, then this connection is direct and very sensitive. We found a highly significant correlation between NDII and S_u, particularly during periods of moisture stress. During dry periods, or during dry spells in the rainy season, as soon as the leaves of the vegetation experience suction pressure, we see high values of the coefficient of determination. Observing the moisture content of vegetation provides us with directly information on the soil moisture state in the root zone. We also found that there is almost no lag time between S_u and NDII. This illustrates the fast response of vegetation to soil moisture variation, which makes the NDII a sensitive and direct indicator for root zone moisture content. In fact, the canopy acts as a kind of manometer for the root zone moisture content.

5.2 The validity of the hypothesis

In natural catchments, it is not possible to prove a hypothesis by using a calibrated model. There are too many factors contributing to the uncertainty of results: the processes are too heterogeneous, the observations are not without error, the climatic drivers are too uncertain and heterogeneous and finally there is substantial model uncertainty, both in the semi-distributed hydrological model and in the remote sensing model used to determine the 8-day NDII product. In this case we have selected a lumped conceptual model, which is good at mimicking the main runoff processes, but which lacks the detail of distributed models. Distributed models, however, require detailed and spatially explicit information (which is missing) and are generally over-parameterized, turning them highly unreliable in data-scarce environments. On top of this there is considerable doubt if they provide the right answers for the right reasons.

This paper is not a modelling study, but a test of the hypothesis whether the observed NDII correlates with the modelled root zone storage. We have seen in Figure 6 that the correlation is strong during periods of moisture stress, but that when the root zone is near saturation the correlation is weak. But we also saw that even in the wet season, during short dry spells, the correlation is strong. Even when the seasonality is removed, the patterns between NDII and S_u in Figure 7 are similar, although there are two dry seasons when this is less the case (in 2004 and 2006). So given the implicit uncertainty of the hydrological model, the uncertainty of the meteorological drivers, as well as the river discharges to which the models have been calibrated, and the uncertainty associated with the relationship between NDII and EWT, the good correspondence between the NDII and the root zone storage of the model during periods of moisture stress support the potential value of the NDII as a proxy for root zone storage in a conceptual model. It is in our view even likely that the differences between the signals of the NDII and the S_u are rather related to model uncertainty, the uncertainty of the climatic drivers, the uncertainty in the relationship between NDII and EWT, and the problems of determining accurate NDII estimates over 8-days periods, than due to a weak correlation between the root zone storage and the NDII.

5.3 Implication in hydrological modelling

Simulation of root zone soil moisture is crucial in hydrological modelling (Houser et al., 1998; Western and Blöschl, 1999). Using estimates of soil moisture states could increase model performance and realism, but moreover, it would be powerful information to facilitate prediction in ungauged basins (Hrachowitz et al., 2013). However, until now, it has not been practical (e.g. Parajka et al., 2006; Entekhabi et al., 2010). Assimilating soil moisture in hydrological models, either from top-soil observation by remote sensing, or from the deeper soil column by models (Reichle, 2008), is still a challenge. Several studies showed how difficult it is to assimilate soil moisture data to improve daily runoff simulation (Parajka et al., 2006; Matgen et al., 2012).

There are several reasons why we have not compared our results with soil moisture observations in the field. Firstly, observations of soil moisture are not widely available. Moreover, it is not straightforward to link classical soil moisture observations to the actual moisture available in the root zone. Most observations are conducted at fixed depths and at certain locations within a highly heterogeneous environment. Without knowing the details of the root distribution, both horizontally and vertically, it is hard, if not impossible, to estimate the water volume accessible to plants through their root systems. We should realize that it is difficult to observe root zone soil moisture even at a local scale. But measuring root zone soil moisture at a catchment scale is even more challenging. State-of-the-art remote sensing techniques can observe spatially distributed soil moisture, but what they can see is only the near-surface layers if not blocked by vegetation. The top layer moisture may or not be correlated with the root zone storage, amongst others depending on the vegetation type, but it is definitely not the same.

By observing the moisture content of the leaves, the NDII represents the soil moisture content of the entire root zone, which is precisely the information that hydrological models require as this is the component that controls the occurrence and magnitude of storage deficits and thereby the moisture dynamics of a system. This study clearly shows the temporal correlation between S_{u} and NDII. From the relationship between NDII and S_{u}, we can directly derive a proxy for the soil moisture state at the actual scale of interest, which can potentially be assimilated in hydrological models. Being such a key state variable, the NDII-derived S_u could become a potentially powerful and otherwise unavailable constraint for the soil moisture component of hydrological models. This would mean a breakthrough in hydrological modelling as it would allow a robust parameterization of water partitioning into evaporative fluxes and drainage even in data scarce environments. Given the implicit uncertainties in hydrological modelling, this new and readily available proxy could potentially enhance our implicitly uncertain modelling practice. More importantly it would open completely new venues for modelling ungauged parts of the world and could become extremely useful for discharge prediction in ungauged basins (Hrachowitz et al., 2013).

We should, of course, be aware of regional limitations. The proxy only appears to work for periods of moisture stress. This study considered a tropical seasonal evergreen ecosystem, where periods of moisture stress regularly occur. In ecosystems which shed their leaves, or go dormant, other conditions may apply. We need further investigations into the usefulness of this approach in catchments with different climates. In addition, the phenology of the ecosystem is of importance, which should be taken into consideration in follow-up research. Finally, a comparison with distributed or semi-distributed models would be a further test of the value of the NDII as proxy for the root zone moisture content.

6. Conclusions

The NDII was used to investigate drought for the UPRB from 2001 to 2013. Monthly average NDII values appear to be spatially distributed over the UPRB, in agreement with seasonal variability and landscape characteristics. NDII values appear to be lower during the dry season and higher during the wet season as a result of seasonal differences between precipitation and evaporation. The NDII appears to correlate well with the moisture content in the root zone, offering a potential proxy variable for calibration of hydrological models in ungauged basins.

To illustrate the importance of NDII as a proxy for root zone moisture content in hydrological models, we applied the FLEX model to assess the root zone soil moisture storage (S_u) of 8 sub-catchments of the UPRB controlled by 8 runoff stations. The results show that the 8-day average NDII values over the study sub-basin correlate well with the 8-day average S_u for all sub-catchments during dry periods (average R^2 equals 0.87), and less so during wet spells (average R^2 equals 0.61). The NDII appears to be a promising proxy for root zone moisture content during dry spells when leaves are under moisture stress. The natural interaction between rainfall, soil moisture, and leave water content can be visualised by the NDII, making it an important indicator both for hydrological modelling and drought assessment.

The potential of using the NDII to constrain model parameters (such as the power of the beta function β, recharge splitter D and C_e in the transpiration function) in ungauged basins is an important new venue, which could potentially facilitate the major question of prediction in ungauged basins.

Acknowledgement

We gratefully acknowledge Kasetsart University Research and Development Institute for financially supporting this research. We also appreciate Royal Irrigation Department and Thai Meteorological Department for providing the rainfall data. Finally, we sincerely thank the MODIS Land Discipline Group for creating and sharing the MODIS LAND data used in this study.

References

Albergel, C., Rüdiger, C., Pellarin, T., Calvet, J. C., Fritz, N., Froissard, F., Suquia, D., Petitpa, A., Piguet, B., and Martin, E.: From near-surface to root-zone soil moisture using an exponential filter: an assessment of the method based on in-situ observations and model simulations, Hydrol. Earth Syst. Sci., 12(6), 1323-1337, 2008.

Beven, K. J. and M. J. Kirkby. 1979. A physically based, variable contributing area model of basin hydrology. Hydrological Sciences Bulletin. 24(1). 43-69.

Ceccato, P., Flasse, S., and Grégoire, J. M.: Designing a spectral index to estimate vegetation water content from remote sensing data: Part 2, Validations and applications, Remote Sens. Environ., 82, 198−207, doi:10.1016/S0034-4257(02)00036-6, 2002.

Ceccato, P., Flasse, S., Tarantola, S., Jacquemoud, S., and Grégoire, J. M.: Detecting vegetation leaf water content using reflectance in the optical domain, Remote Sens. Environ., 77, 22– 33, doi:10.1016/S0034-4257(01)00191-2, 2001.

Cheng, Y. B., Zarco-Tejada, P. J., Riaño, D., Rueda, C. A., and Ustin, S. L.: Estimating vegetation water content with hyperspectral data for different canopy scenarios: Relationships between AVIRIS and MODIS indexes, Remote Sens. Environ., 105, 354–366, doi:10.1016/j.rse.2006.07.005, 2006.

de Groen, M. M., and Savenije, H. H. G.: A monthly interception equation based on the statistical characteristics of daily rainfall, Water Resour. Res., 42, W12417, doi:10.1029/2006WR005013, 2006.

De Jeu, R. A. M., Wagner, W., Holmes, T. R. H., Dolman, A. J., van de Giesen, N. C., and Friesen, J.: Global Soil Moisture Patterns Observed by Space Borne Microwave Radiometers and Scatterometers, Surv. Geophys., 28, 399–420, doi 10.1007/s10712-008-9044-0, 2008.

Entekhabi, D., Nioku, E. G., O'Neill, P. E., Kellogg, K. H., Crow, W. T., Edelstein,W. N., Entin, J. K., Goodman, S. D., Jackson, T. J., Johnson, J., Kimball, J., Piepmeier, J. R., Koster, R. D., Martin, N., McDonald, K. C., Moghaddam, M., Moran, S., Reichle, R., Shi, J.-C., Spencer, M. W., Thurman, S. W., Leung, T., and Van Zyl, J.: The Soil Moisture Active Passive (SMAP) Mission, Proc. IEEE., 98, 704–716, 2010.

Fenicia, F., Kavetski, D., and Savenije, H. H. G.: Elements of a flexible approach for conceptual hydrological modeling: 1. Motivation and theoretical development, Water Resour. Res., 47, W11510, doi:10.1029/2010WR010174, 2011.

Fensholt, R., and Sandholt, I.: Derivation of a shortwave infrared stress index from MODIS near- and shortwave infrared data in a semiarid environment, Remote Sens. Environ., 87, 111−121, doi:10.1016/j.rse.2003.07.002, 2003.

Ford, T. W., Harris, E., and Quiring, S. M.: Estimating root zone soil moisture using near-surface observations from SMOS, Hydrol. Earth Syst. Sci., 18(1), 139-154, 2014.

Friesen, J., Steele-Dunne, S. C., and van de Giesen, N.: Diurnal Differences in Global ERS Scatterometer Backscatter Observations of the Land Surface, IEEE Transactions on Geoscience and Remote Sensing, vol. 50, issue 7, pp. 2595-2602, 2012.

Gao, B. C.: NDWI - A normalized difference water index for remote sensing of vegetation liquid water from space, Remote Sens. Environ., 58, 257−266, doi:10.1016/S0034-4257(96)00067-3, 1996.

Gao, B. C., and Goetz, A. F. H.: Retrieval of equivalent water thickness and information related to biochemical components of vegetation canopies from AVIRIS data, Remote Sens. Environ., 52, 155−162, doi:10.1016/0034-4257(95)00039-4, 1995.

Gao, H., Hrachowitz, M., Fenicia, F., Gharari, S., and Savenije, H. H. G.: Testing the realism of a topography driven model (Flex-Topo) in the nested catchments of the Upper Heihe, China, Hydrol. Earth Syst. Sci., 18, 1895−1915, doi:10.5194/hess-18-1895-2014, 2014(a).

Gao, H., Hrachowitz, M., Schymanski, S. J., Fenicia, F., Sriwongsitanon, N., and Savenije, H. H. G.: Climate controls how ecosystems size the root zone storage capacity at catchment scale, Geophys. Res. Lett., 41, 7916−7923, doi:10.1002/2014GL061668, 2014(b).

Gupta, H. V., Kling, H., Yilmaz, K. K., and Martinez, G. F.: Decomposition of the mean squared error and NSE performance criteria: implications for improving hydrological modeling, J. Hydrol., 377, 80–91, http://dx.doi.org/10.1016/j.jhydrol.2009.08.003, 2009.

Hardisky, M. A., V. Klemas, and R. Michael Smart. "The influence of soil salinity, growth form, and leaf moisture on the spectral radiance of Spartina alterniflora canopies." Photogrammetric Engineering and Remote Sensing 49 (1983): 77-83.

Hargreaves GH, Samani ZA: Reference crop evapotranspiration from temperature. Appl Engine Agric. 1(2):96–99, 1985.

Houser, P. R., Shuttleworth, W. J., Famiglietti, J. S., Gupta, H. V., Syed, K. H., and Goodrich, D. C.: Integration of soil moisture remote sensing and hydrologic modeling using data assimilation, edited, 1998.

Hunt, E. R. Jr. and Rock, B. N.: Detection of changes in leaf water content using near- and middle-infrared reflectances, Remote Sens. Environ., 30, 43–54, doi:10.1016/0034-4257(89)90046-1, 1989.

Hrachowitz, M., Savenije, H.H.G., Blöschl, G., McDonnell, J.J., Sivapalan, M., Pomeroy, J.W., Arheimer, B., Blume, T., Clark, M.P., Ehret, U., Fenicia, F., Freer, J.E., Gelfan, A., Gupta, H.V., Hughes, D.A., Hut, R.W., Montanari, A., Pande, S., Tetzlaff, D., Troch, P.A., Uhlenbrook, S., Wagener, T., Winsemius, H.C., Woods, R.A., Zehe, E., and Cudennec, C.: A decade of Predictions in Ungauged Basins (PUB); a review. Hydrol. Sci. J., 58 (6), 1–58, doi: 10.1080/02626667.2013.803183, 2013.

Hewlett, J.D. and Hibbert, A.R. 1967. Factors affecting the response of small watersheds to precipitation in humid regions. IN Forest Hydrology (eds. W.E. Sopper and H.W. Lull). Pergamon Press, Oxford. pp. 275-290.

Korres, W., Reichenau, T. G., Fiener, P., Koyama, C. N., Bogena, H. R., Cornelissen, T., Baatz, R., Herbst, M., Diekkrüger, B., Vereecken, H., and Schneider, K.: Spatio-temporal soil moisture patterns – A meta-analysis using plot to catchment scale data, J. Hydrol., 520, 326–341, doi:10.1016/j.jhydrol.2014.11.042, 2015.

Jackson, T. J., and Schmugge, T. J.: Vegetation effects on the microwave emission of soils, Remote Sens. Environ., 36(3), 203-212, 1991.

Kerr, Y. H., Waldteufel, P., Wigneron, J.-P., Martinuzzi, J.-M., Font, J., and Berger, M.: Soil Moisture Retrieval from Space: The Soil Moisture and Ocean Salinity (SMOS) Mission, IEEE Transactions on Geoscience and Remote Sensing, 39(8), 1729-1735, 2001.

Legates, D. R., Mahmood, R., Levia, D. F., DeLiberty, T. L., Quiring, S. M., Houser, C., and Nelson, F. E.: Soil moisture: A central and unifying theme in physical geography, Prog. Phys. Geogr., 35, 65–86, 2011.

Liang, X., Lettenmaier, D. P., Wood, E. F., and Burges, S. J.: A simple hydrologically based model of land surface water and energy fluxes for general circulation models, Journal of Geophysical Research: Atmospheres, 99, 14 415-14 428, 1994.

Mahmood, R., and Hubbard, K. G.: Relationship between soil moisture of near surface and multiple depths of the root zone under heterogeneous land uses and varying hydroclimatic conditions, Hydrological Processes, 25, 3449-3462, doi: 10.1002/hyp.6578, 2004.

Mapiam, P. P., Sharma, A., and Sriwongsitanon, N.: Defining the Z~R relationship using gauge rainfall with coarse temporal resolution: Implications for flood forecast. J. Hydrol. Eng., 19, 04014004, doi: 10.1061/(ASCE)HE.1943-5584.0000616, 2014.

Mapiam, P. P., and Sriwongsitanon, N.: Estimation of the URBS model parameters for flood estimation of ungauged catchments in the upper Ping river basin, Thailand. ScienceAsia, 35, 49–56, 2009.

Matgen P, Fenicia F, Heitz S, Plaza D, de Keyser R, Pauwels VRN, et al. Can ASCAT-derived soil wetness indices reduce predictive uncertainty in well-gauged areas? A comparison with in situ observed soil moisture in an assimilation application. Adv Water Resour 2012;44:49–65. doi:http://dx.doi.org/10.1016/j.advwatres.2012.03.022.

Parajka, J., Naeimi, V., Blöschl, G., Wagner, W., Merz, R., and Scipal, K.: Assimilating scatterometer soil moisture data into conceptual hydrologic models at the regional scale, Hydrol. Earth Syst. Sci., 10(3), 353-368, 2006.

Peñuelas, J., Filella, I., Biel, C., Serrano, L., and Savé, R.: The reflectance at the 950–970 nm region as an indicator of plant water status, Int. J. Remote Sens., 14, 1887–1905, doi:10.1080/01431169308954010, 1993.

Porporato, A., Daly, E., and Rodriguez-Iturbe, I.: Soil water balance and ecosystem response to climate change, The American Naturalist, 164, 625-623, 2004.

Reichle, R. H.: Data assimilation methods in the Earth sciences, Adv. Water Resour., 31(11), 1411-1418, 2008.

Rutter, A. J., and Sands, K. (1958). The relation of leaf water deficit to soil moisture tension in Pinus sylvestris, L. 1. The effect of soil moisture on diurnal change in water balance. New Phytol. 57: 50--65.

Schaefli, B., & Gupta, H. V. Do Nash values have value?. Hydrological Processes, 21(15), 2075-2080, 2007.

Shi, J., Wang, J., Hsu, A. Y., O'Neill, P. E., and Engman, E. T.: Estimation of bare surface soil moisture and surface roughness parameter using L-band SAR image data, Geoscience and Remote Sensing, IEEE Transactions on, 35(5), 1254-1266, 1997.

Shukla, J., & Mintz, Y. (1982). Influence of land-surface evapotranspiration on the earth’s climate. Science, 215(4539), 1498-1501.

Sriwongsitanon, N.: Flood forecasting system development for the Upper Ping River Basin. Kasetsart Journal (Natural Science), 44(4), 2010.

Sriwongsitanon, N. and Taesombat, W.: Effects of land cover on runoff coefficient, J. Hydrol., 410, 226–238, doi:10.1016/j.jhydrol.2011.09.021, 2011.

Steele-Dunne, S. C., Friesen, J., and van de Giesen, N.: Using Diurnal Variation in Backscatter to Detect Vegetation Water Stress, IEEE Transactions on Geoscience and Remote Sensing, vol. 50, issue 7, pp. 2618-2629, 2012.

Tucker, C. J.: Remote sensing of leaf water content in the near infrared, Remote Sens. Environ., 10, 23–32, doi:10.1016/0034-4257(80)90096-6, 1980.

Ustin, S. L., Roberts, D. A., Gamon, J. A., Asner, G. P. and Green, R. O.: Using Imaging Spectroscopy to Study Ecosystem Processes and Properties. BioScience, 54, 523–534, doi:10.1641/0006-3568(2004)054[0523:UISTSE]2.0.CO;2, 2004.

Van Emmerik, T., Steele-Dunne, S.C., Judge, J. and van de Giesen, N.C.: Impact of Diurnal Variation in Vegetation Water Content on Radar Backscatter From Maize During Water Stress, IEEE Transactions on Geoscience and Remote Sensing, vol. 53, issue 7, doi:10.1109/TGRS.2014.2386142, 2015.

Vermote, E. F., Kotchenova, S. Y., and Ray, J. P.: MODIS Surface Reflectance User's Guide. Web site: http://modis-sr.ltdri.org, 2011.

Vrugt, J. A., Gupta, H. V., Bastidas, L. A., Bouten, W. and Sorooshian, S.: Effective and efficient algorithm for multiobjective optimization of hydrologic models, Water Resour. Res., 39, 1214. doi:10.1029/2002WR001746, 2003.

Western, A. W., and Blöschl, G.: On the spatial scaling of soil moisture, J. Hydrol., 217(3–4), 203-224, 1999.

Yilmaz, M. T., Hunt, E. R. Jr., and Jackson, T. J.: Remote sensing of vegetation water content from equivalent water thickness using satellite imagery, Remote Sens. Environ., 112, 2514–2522, doi:10.1016/j.rse.2007.11.014, 2008.

Zhao, R. J.: The Xinanjiang model applied in China, J. Hydrol., 135, 371–381, doi:10.1016/0022-1694(92)90096-E, 1992.

Table 1. Catchment characteristics and data period for selected 8 sub-basins in the UPRB.

Sub-basin	Mae Taeng at Ban Mae Taeng (P.4A)	Nam Mae Chaem at Kaeng Ob Luang (P.14)	Ping River at Chiang Dao (P.20)	Nam Mae Rim at Ban Rim Tai (P.21)	Nam Mae Klang at Pracha Uthit Bridge (P.24A)	Nam Mae Khan at Ban Klang (P.71)	Nam Mae Li at Ban Mae E Hai (P.76)	Nam Mae Tha at Ban Sop Mae Sapuad (P.77)
Area (km^2)	1902	3853	1355	515	460	1771	1541	547
Altitude range (m)	1020	991	790	731	888	828	618	641
Average channel slope (%)	0.78	0.81	0.80	0.72	0.98	0.69	0.41	0.63
Average forest and agricultural areas (%)	81.9, 16.5	91.8, 7.4	80.9, 12.8	86.1, 11.6	79.7, 14.2	86.1, 10.1	69.7, 20.1	80.4, 12.7
Average rainfall depth (wet season/ dry season) (mm)	953 (88%) 130 (12%)	883 (92%) 75 (8%)	1076 (88%) 150 (12%)	1019 (90%) 115 (10%)	860 (88%) 121(12%)	1090 (89%) 132 (11%)	1092 (91%) 106 (9%)	757 (88%) 88 (10%)
Number of years data is coincident with NDII	11	7	12	11	12	9	12	12
Data period	1995-2011	1995-2007	1995-2012	1995-2011	1995-2012	1996-2009	1996-2012	1996-2012

Table 2. Water balance and constitutive equations used in FLEX[L].

Reservoirs	Water balance equations	Equation	Constitutive equations	Equation
Interception	$\frac{\mathrm{d}S_\mathrm{i}}{\mathrm{d}t}=P-E_\mathrm{i}-P_\mathrm{e}$	(2)	$E_\mathrm{i}=\begin{cases}E_0; S_\mathrm{i}>0\\0; S_\mathrm{i}=0\end{cases}$	(3)
			$P_\mathrm{e}=\begin{cases}0; S_\mathrm{i}<S_\mathrm{i,max}\\P; S_\mathrm{i}=S_\mathrm{i,max}\end{cases}$	(4)
Root zone reservoir	$\frac{\mathrm{d}S_\mathrm{u}}{\mathrm{d}t}=P_\mathrm{e}-R-E_\mathrm{t}$	(5)	$\frac{R}{P_\mathrm{e}}=1-(1-\frac{S_\mathrm{u}}{(1+\beta)S_\mathrm{u,max}})^\beta$	(6)
			$E_t=(E_0-E_\mathrm{i})\cdot\min(1,\frac{S_\mathrm{u}}{C_\mathrm{e}S_\mathrm{u,max}(1+\beta)})$	(7)
Splitter and Lag function			$R_\mathrm{f}=R\cdot D$	(8)
			$R_\mathrm{s}=R\cdot(1-D)$	(9)
			$R_\mathrm{fl}(t)=\sum_{i=1}^{T_\mathrm{lag}}c(i)\cdot R_\mathrm{f}(t-i+1)$	(10)
			$c(i)=i/\sum_{u=1}^{T_\mathrm{lag}}u$	(11)
Fast reservoir	$\frac{\mathrm{d}S_\mathrm{f}}{\mathrm{d}t}=R_\mathrm{fl}-Q_\mathrm{ff}-Q_\mathrm{f}$	(12)	$Q_\mathrm{ff}=\max(0,S_\mathrm{f}-S_\mathrm{f,max})/K_\mathrm{ff}$	(13)
			$Q_\mathrm{f}=S_\mathrm{f}/K_\mathrm{f}$	(14)
Slow reservoir	$\frac{\mathrm{d}S_\mathrm{s}}{\mathrm{d}t}=R_\mathrm{s}-Q_\mathrm{s}$	(15)	$Q_\mathrm{s}=S_\mathrm{s}/K_\mathrm{s}$	(16)

Table 3. Parameter ranges of the FLEX Model.

Parameter	Range	Parameters	Range
$S_{i,max}$ (mm)	(0.1, 6)	K_{ff} (d)	(1, 9)
$S_{u,max}$ (mm)	(10, 1000)	T_{lagF} (d)	(0, 5)
β (-)	(0, 2)	T_{lagS} (d)	(0, 5)
C_e (-)	(0.1, 0.9)	K_f (d)	(1, 40)
D (-)	(0, 1)	K_s (d)	(10, 500)
$S_{f,max}$ (mm)	(10, 200)		

Table 4. Average NDII values during the wet season, the dry season, and the whole year from 2001 to 2013, and their order of moisture content (Range from 1 to 13. Less value indicates less NDII) for the entire Upper Ping River Basin.

Year	Wet season (May-October)	Dry season (November-April)	Annual
2001-2002	0.223 (2)	0.119 (7)	0.171 (4)
2002-2003	0.205 (9)	0.149 (1)	0.177 (1)
2003-2004	0.218 (5)	0.091 (12)	0.155 (12)
2004-2005	0.210 (8)	0.088 (13)	0.149 (13)
2005-2006	0.200 (11)	0.128 (3)	0.164 (7)
2006-2007	0.224 (1)	0.111 (10)	0.168 (5)
2007-2008	0.222 (3)	0.130 (2)	0.176 (2)
2008-2009	0.221 (4)	0.123 (5)	0.172 (3)
2009-2010	0.213 (7)	0.101 (11)	0.157 (11)
2010-2011	0.197 (13)	0.128 (4)	0.163 (8)
2011-2012	0.216 (6)	0.116 (9)	0.166 (6)
2012-2013	0.201 (10)	0.118 (8)	0.159 (10)
2013-2014	0.199 (12)	0.123 (6)	0.161 (9)
Average	0.211	0.118	0.165
Maximum	0.224	0.149	0.177
Minimum	0.197	0.088	0.149

Table 5. Monthly average NDII values between 2001 and 2013 and the order of basin moisture content for each of 14 sub-basins within the UPRB.

Sub-basin	Jan	Feb	Mar	Apr	May	Jun	Jul	Aug	Sep	Oct	Nov	Dec	Average
Ping River Section 1	0.14 (7.5)	0.06 (7.4)	0.02 (8.8)	0.07 (8.9)	0.17 (8.4)	0.21 (6.2)	0.22 (4.5)	0.22 (6.1)	0.24 (7.5)	0.23 (8.3)	0.22 (7.8)	0.18 (7.2)	0.16 (8)
Nam Mae Ngad	0.17 (5.2)	0.11 (5.9)	0.07 (6.2)	0.10 (6.3)	0.18 (6.9)	0.21 (7.1)	0.21 (7.5)	0.22 (8.0)	0.23 (9.2)	0.23 (7.9)	0.23 (6.4)	0.20 (5.7)	0.18 (6)
Nam Mae Taeng	0.21 (1.3)	0.16 (1.0)	0.13 (1.2)	0.14 (2.1)	0.19 (3.9)	0.21 (6.1)	0.22 (6.0)	0.23 (4.5)	0.25 (3.1)	0.25 (2.6)	0.26 (1.2)	0.24 (1.7)	0.21 (1)
Ping River Section 2	0.07 (11.5)	0.02 (9.8)	0.01 (9.2)	0.04 (11.6)	0.13 (13.1)	0.18 (13.0)	0.18 (13.5)	0.19 (13.3)	0.21 (13.6)	0.21 (12.7)	0.17 (13.4)	0.12 (13.5)	0.13 (12)
Nam Mae Rim	0.17 (5.3)	0.13 (4.3)	0.10 (3.9)	0.13 (3.3)	0.20 (2.6)	0.22 (3.7)	0.22 (4.0)	0.24 (2.5)	0.26 (1.3)	0.26 (1.2)	0.24 (3.7)	0.20 (5.6)	0.20 (2)
Nam Mae Kuang	0.09 (9.4)	0.03 (9.5)	0.02 (9.3)	0.05 (10.1)	0.15 (10.0)	0.20 (8.1)	0.21 (8.1)	0.22 (8.2)	0.24 (7.0)	0.23 (7.5)	0.20 (10.4)	0.14 (10.7)	0.15 (9)
Nam Mae Ngan	0.18 (4.0)	0.13 (4.4)	0.10 (4.9)	0.13 (4.1)	0.19 (3.9)	0.21 (5.3)	0.22 (5.5)	0.23 (5.2)	0.25 (3.9)	0.24 (4.5)	0.24 (4.5)	0.22 (4.0)	0.19 (5)
Nam Mae Li	0.05 (12.5)	-0.04 (12.5)	-0.04 (12.7)	0.02 (12.1)	0.14 (11.9)	0.19 (11.8)	0.20 (9.7)	0.23 (8.3)	0.23 (9.9)	0.21 (13.0)	0.18 (13.2)	0.13 (12.5)	0.12 (13)
Nam Mae Klang	0.19 (3.3)	0.13 (3.5)	0.12 (2.8)	0.14 (2.3)	0.20 (2.9)	0.22 (4.8)	0.22 (7.2)	0.23 (7.6)	0.23 (8.6)	0.24 (7.2)	0.24 (4.5)	0.22 (3.3)	0.20 (4)
Ping River Section 3	0.06 (11.7)	-0.03 (12.5)	-0.04 (12.3)	0.03 (11.2)	0.15 (9.3)	0.21 (7.2)	0.21 (8.7)	0.21 (9.9)	0.22 (11.4)	0.21 (11.9)	0.19 (11.2)	0.15 (10.3)	0.13 (11)
Upper Nam Mae Chaem	0.20 (1.9)	0.15 (2.0)	0.12 (2.3)	0.13 (4.2)	0.18 (6.7)	0.20 (9.5)	0.21 (9.2)	0.21 (9.1)	0.24 (6.2)	0.25 (3.9)	0.26 (2.1)	0.24 (1.6)	0.20 (3)
Lower Nam Mae Chaem	0.09 (9.8)	0.006 (10.7)	-0.007 (10.8)	0.05 (10.2)	0.15 (10.2)	0.20 (10.2)	0.20 (9.9)	0.21 (8.9)	0.23 (9.5)	0.23 (8.3)	0.21 (8.9)	0.16 (9.2)	0.14 (10)
Nam Mae Haad	0.03 (14.0)	-0.07 (14.0)	-0.06 (13.8)	0.003 (12.9)	0.15 (10.0)	0.21 (5.8)	0.22 (6.4)	0.23 (6.2)	0.24 (5.2)	0.22 (9.7)	0.19 (11.2)	0.12 (12.4)	0.12 (14)
Nam Mae Tuen	0.13 (7.6)	0.05 (7.7)	0.05 (7.0)	0.10 (5.9)	0.19 (5.2)	0.21 (6.2)	0.22 (4.9)	0.222 (7.2)	0.23 (8.7)	0.24 (6.2)	0.23 (6.5)	0.20 (6.5)	0.17 (7)
Average	0.13	0.06	0.04	0.08	0.17	0.20	0.21	0.22	0.24	0.23	0.22	0.18	0.16
Maximum	0.21	0.16	0.13	0.14	0.20	0.22	0.22	0.24	0.26	0.26	0.26	0.24	0.21
Minimum	0.03	-0.07	-0.06	0.003	0.13	0.18	0.18	0.19	0.21	0.21	0.17	0.12	0.12

Table 6. FLEX parameters calibrated at 8 runoff stations located in the UPRB.

Runoff station	$S_{i,max}$ (mm)	$S_{u,max}$ (mm)	C_e (-)	β (-)	D (-)	K_f (days)	K_s (days)	T_{lagF} (days)	T_{lagS} (days)	$S_{f,max}$ (mm)	K_{ff} (days)
P.4A	2.0	463	0.30	0.66	0.77	2.9	42	1.1	49	93	9.1
P.14	2.3	269	0.55	1.16	0.65	4.0	63	1.5	39	155	7.6
P.21	2.3	388	0.31	0.90	0.64	2.1	66	2.4	48	33	2.5
P.20	2.0	324	0.47	0.50	0.79	7.7	103	1.0	25	69	1.7
P.24A	3.2	209	0.77	1.53	0.89	3.2	267	1.5	44	24	4.2
P.76	2.3	486	0.62	0.32	0.89	2.4	191	2.7	3	130	7.4
P.77	4.5	344	0.48	0.27	0.75	1.5	65	1.2	30	164	5.6
P.71	4.3	532	0.34	0.46	0.90	3.5	80	1.8	15	179	6.5

Table 7. FLEX model performance at 8 runoff stations.

Station	Data period	I_{KGE}	I_{KGL}	I_{KGF}
P.4A	1995-2009	0.822	0.667	0.963
P.14	1995-2007	0.796	0.442	0.966
P.21	1995-2009	0.814	0.718	0.985
P.20	1995-2011	0.792	0.685	0.964
P.24A	1995-2011	0.623	0.598	0.945
P76	2000-2011	0.539	0.665	0.916
P.77	1999-2011	0.775	0.612	0.970
P.71	1996-2009	0.823	0.714	0.975
Average		0.748	0.638	0.961

Table 8. Exponential relationships between the average NDII values and simulated root zone moisture storage (S_u) in the 8 sub-basins controlled by the 8 runoff stations.

Runoff station	Annual Relationship			Wet Season Relationship			Dry Season Relationship		
	a	b	R^2	a	b	R^2	a	b	R^2
P.4A	11.2	12.4	0.66	11.1	12.9	0.53	12.6	11.2	0.90
P.14	21.9	9.8	0.81	19.2	10.8	0.71	24.6	8.5	0.92
P.20	52.3	7.4	0.79	36.2	9.1	0.72	59.7	6.7	0.91
P.21	30.8	9.0	0.68	27.8	9.3	0.53	30.6	9.22	0.86
P.24A	22.1	8.5	0.60	24.2	8.3	0.41	22.4	8.1	0.81
P.71	2.1	19.9	0.77	1.9	20.5	0.65	2.3	19.0	0.87
P.76	10.1	13.6	0.85	8.1	14.4	0.74	10.8	14.6	0.87
P.77	35.4	8.0	0.70	20.7	10.2	0.61	40.6	7.7	0.83
Average	-	-	0.73	-	-	0.61	-	-	0.87

Note: $S_u = ae^{bNDII}$

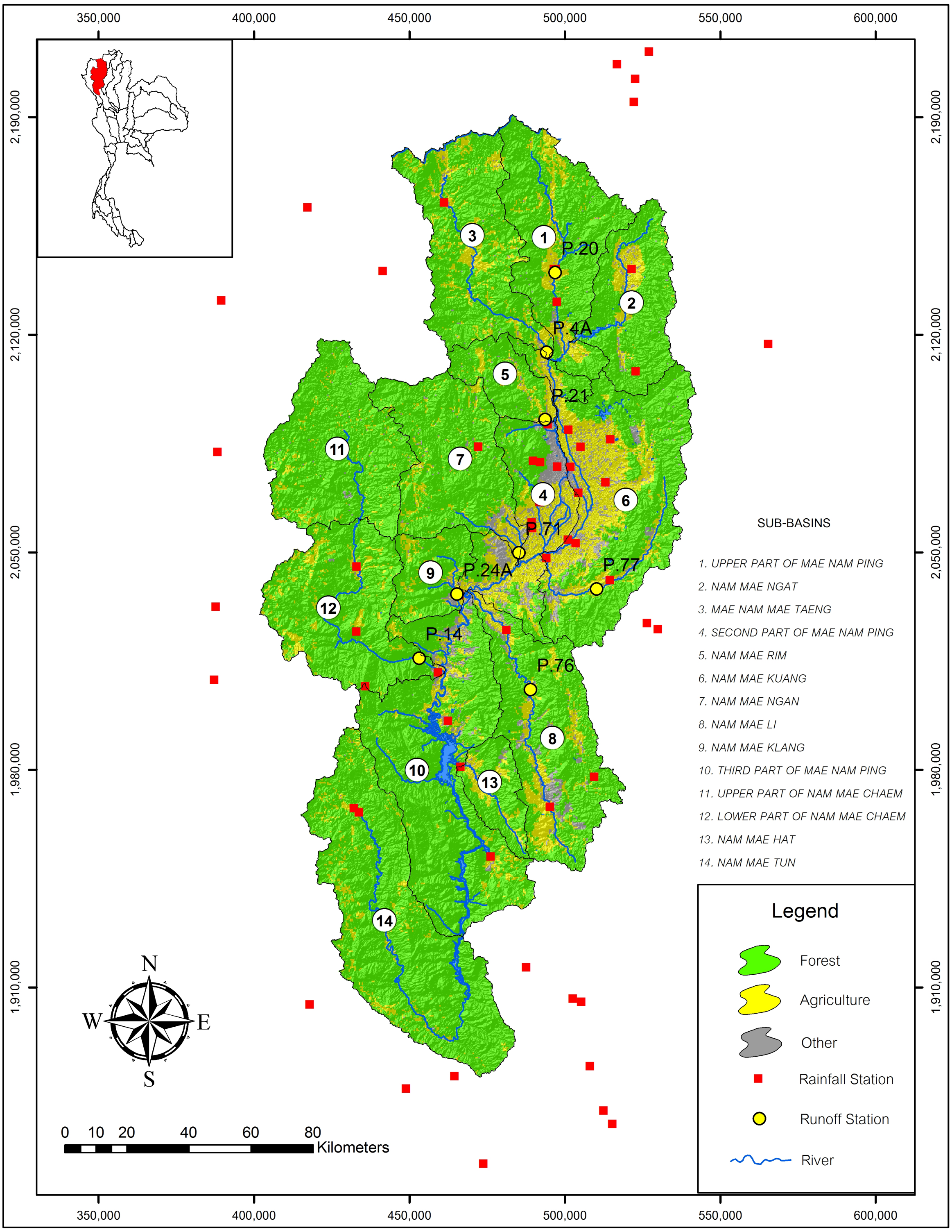

Figure 1. The Upper Ping River Basin (UPRB) and the locations of the rain-gauge and runoff stations. The numbers indicate the 14 sub-basins of the UPRB.

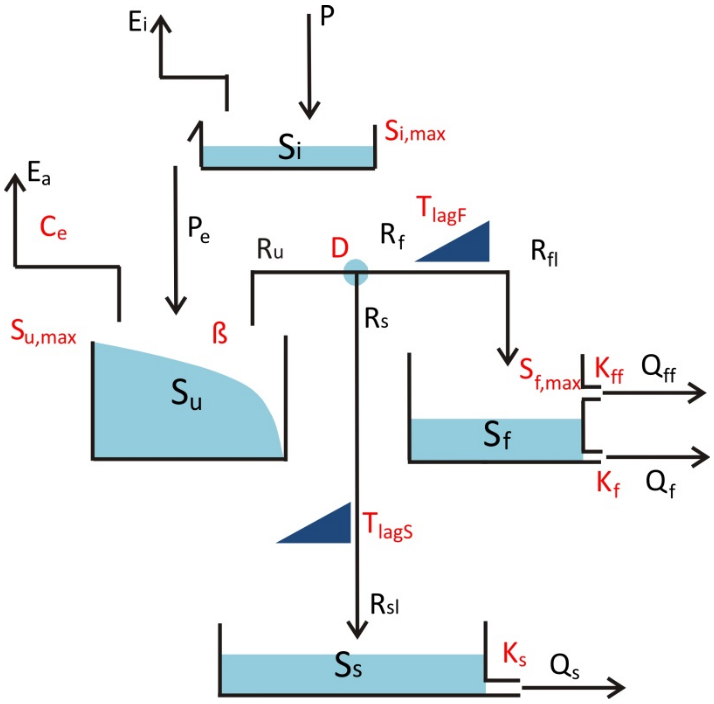

Figure 2. Model structure of the FLEX.

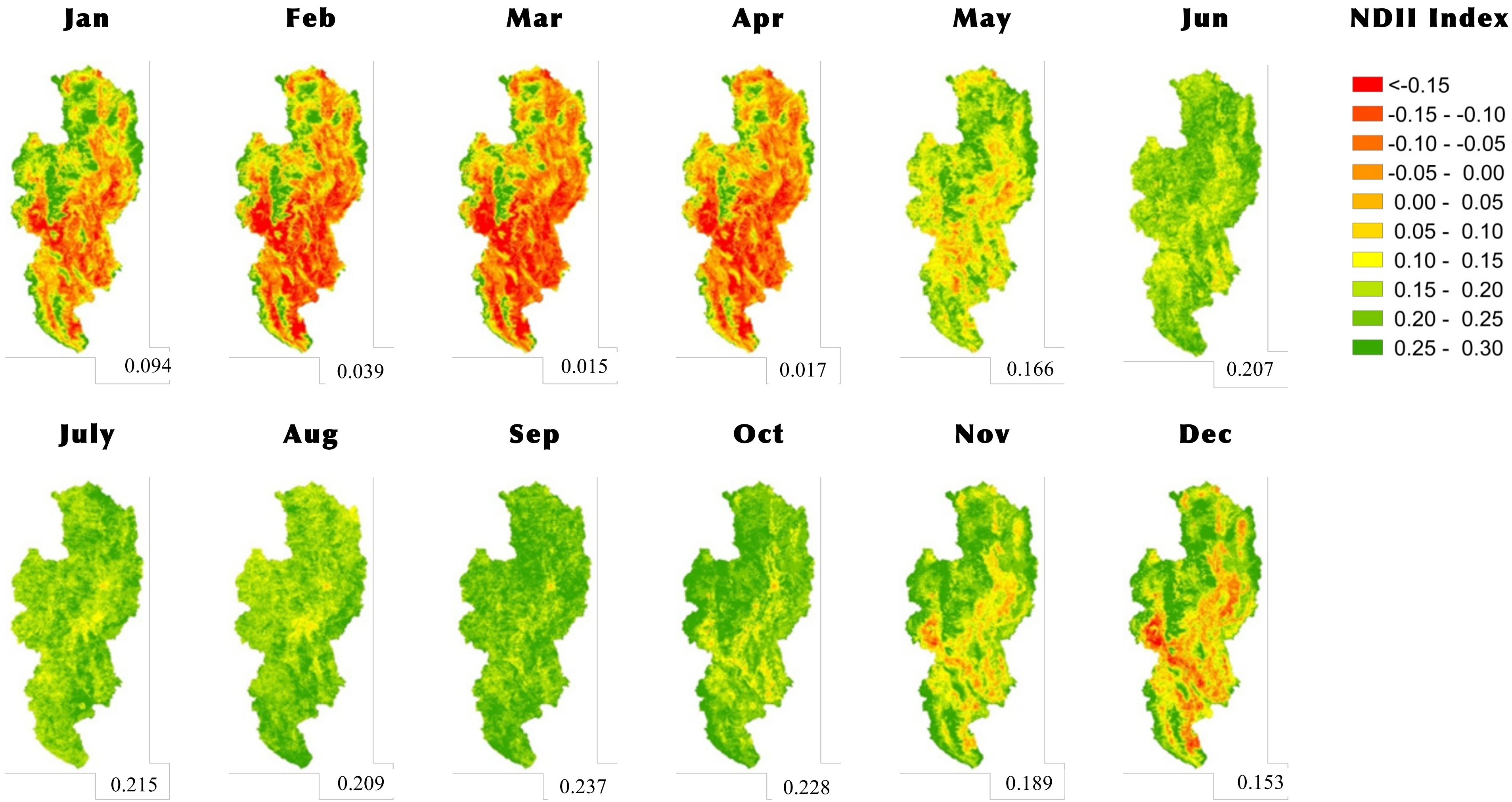

Figure 3. Monthly average NDII values for the UPRB in 2004. The green color indicates an NDII between 0.15 and 0.30, yellow between 0 and 0.15, orange between -0.15 and 0 and red an NDII<-0.15) representing relatively high-, medium-, low-, and very low- root zone moisture content.

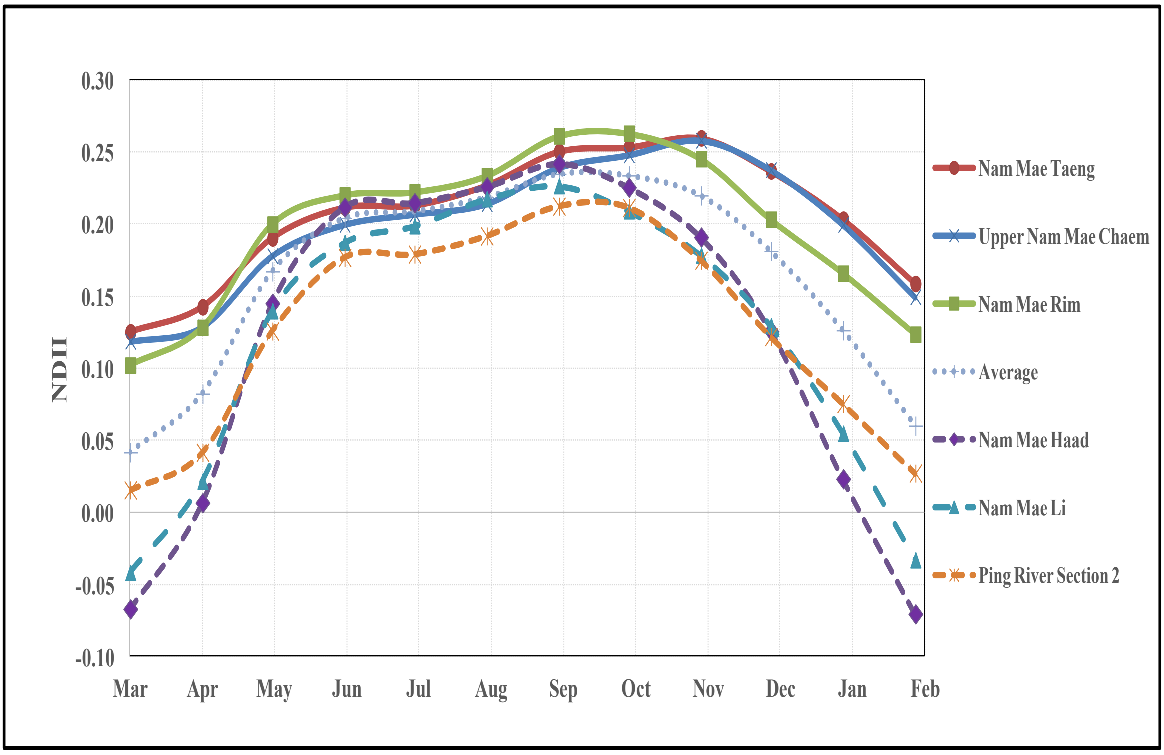

Figure 4. Monthly average NDII values for 6 sub-basins compared to the basin average in the UPRB. Note that three wettest and three driest basins are presented in this graph.

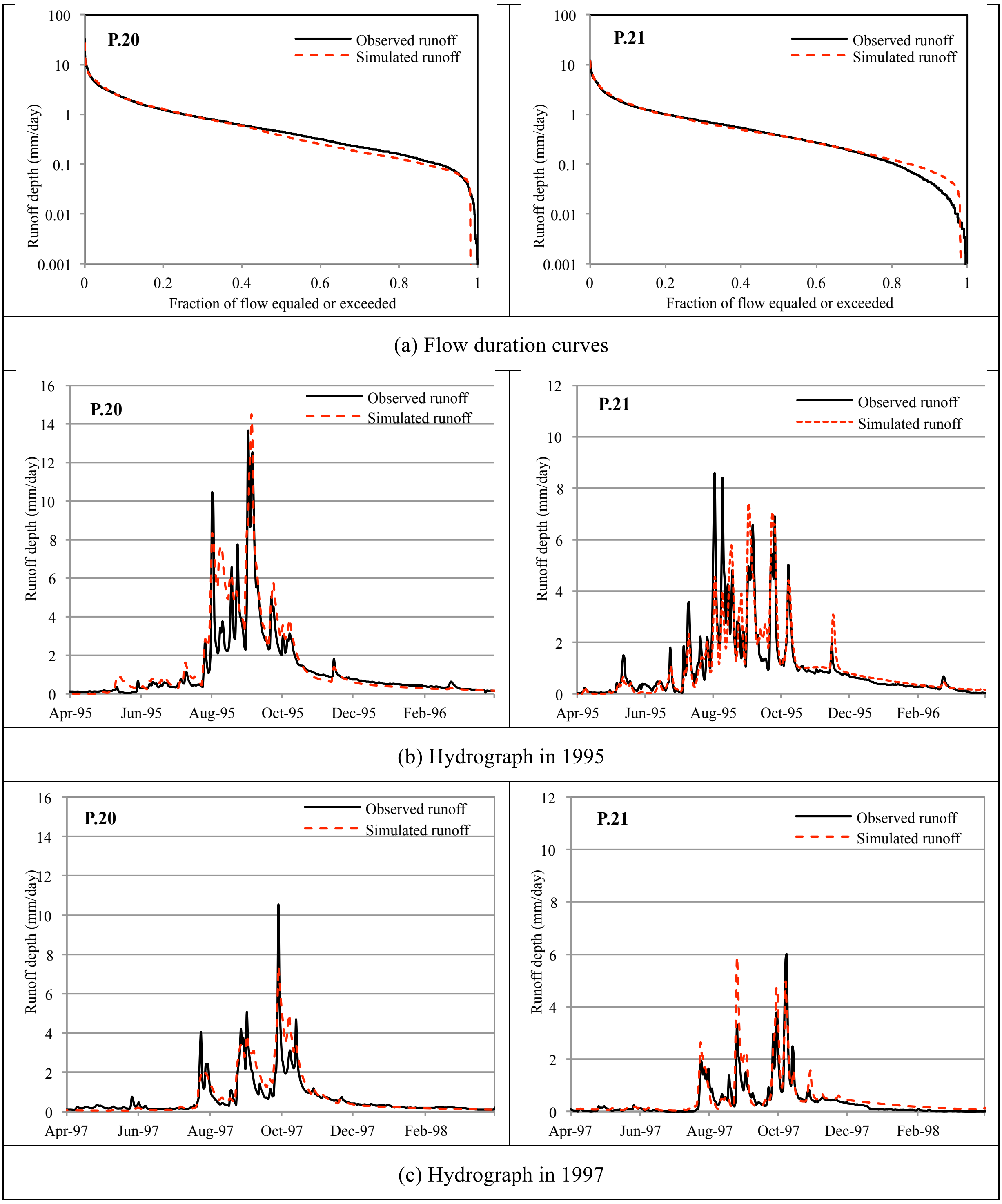

Figure 5. Examples of flow duration curves and simulated hydrographs using FLEX at runoff stations P.20 and P.21.

<table>
<tr><th>Runoff Station</th><th>Annual</th><th>Wet Season</th><th>Dry Season</th></tr>
<tr><td>P.4A</td>
<td>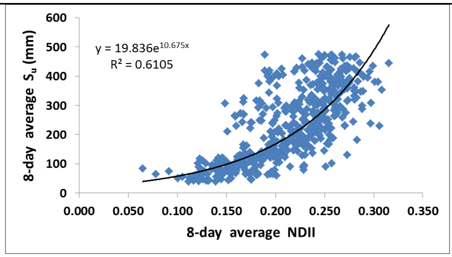
</td>
<td>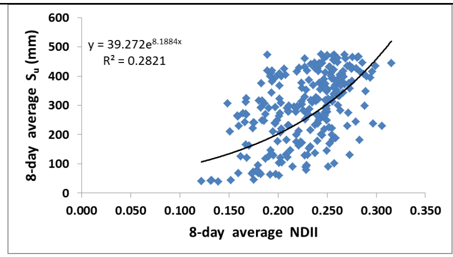
</td>
<td>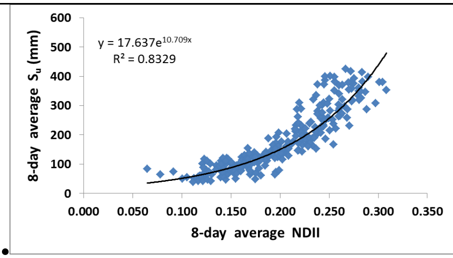
</td></tr>
<tr><td>P.14</td>
<td>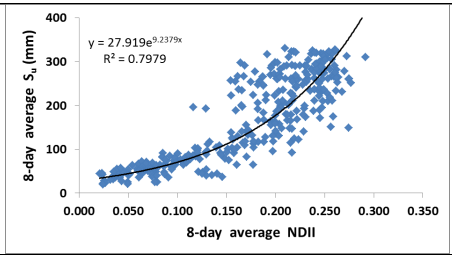
</td>
<td>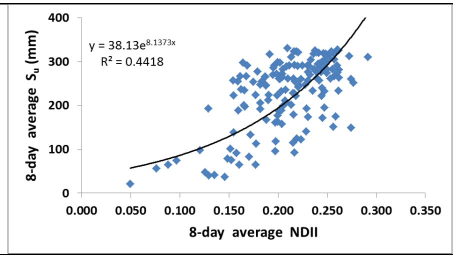
</td>
<td>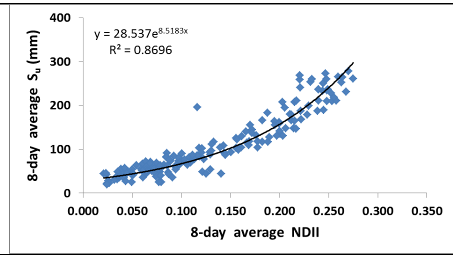
</td></tr>
<tr><td>P.20</td>
<td>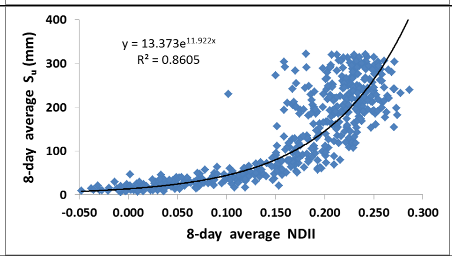
</td>
<td>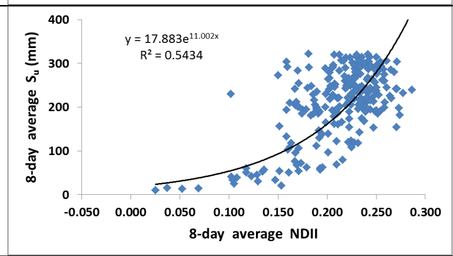
</td>
<td>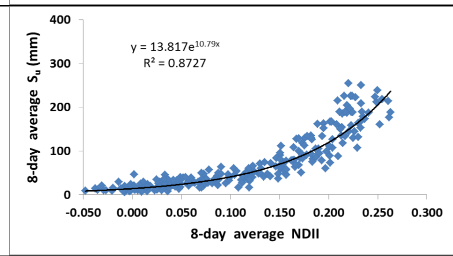
</td></tr>
<tr><td>P.21</td>
<td>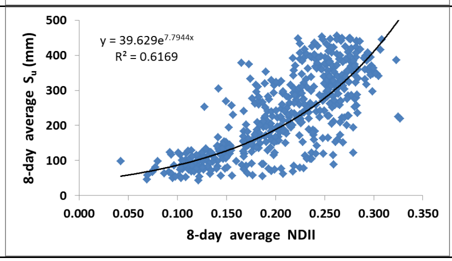
</td>
<td>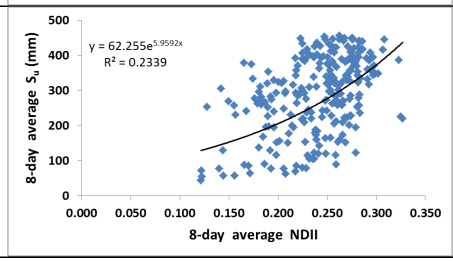
</td>
<td>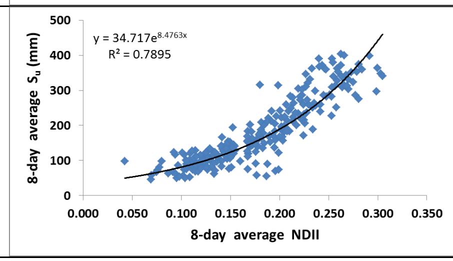
</td></tr>
</table>

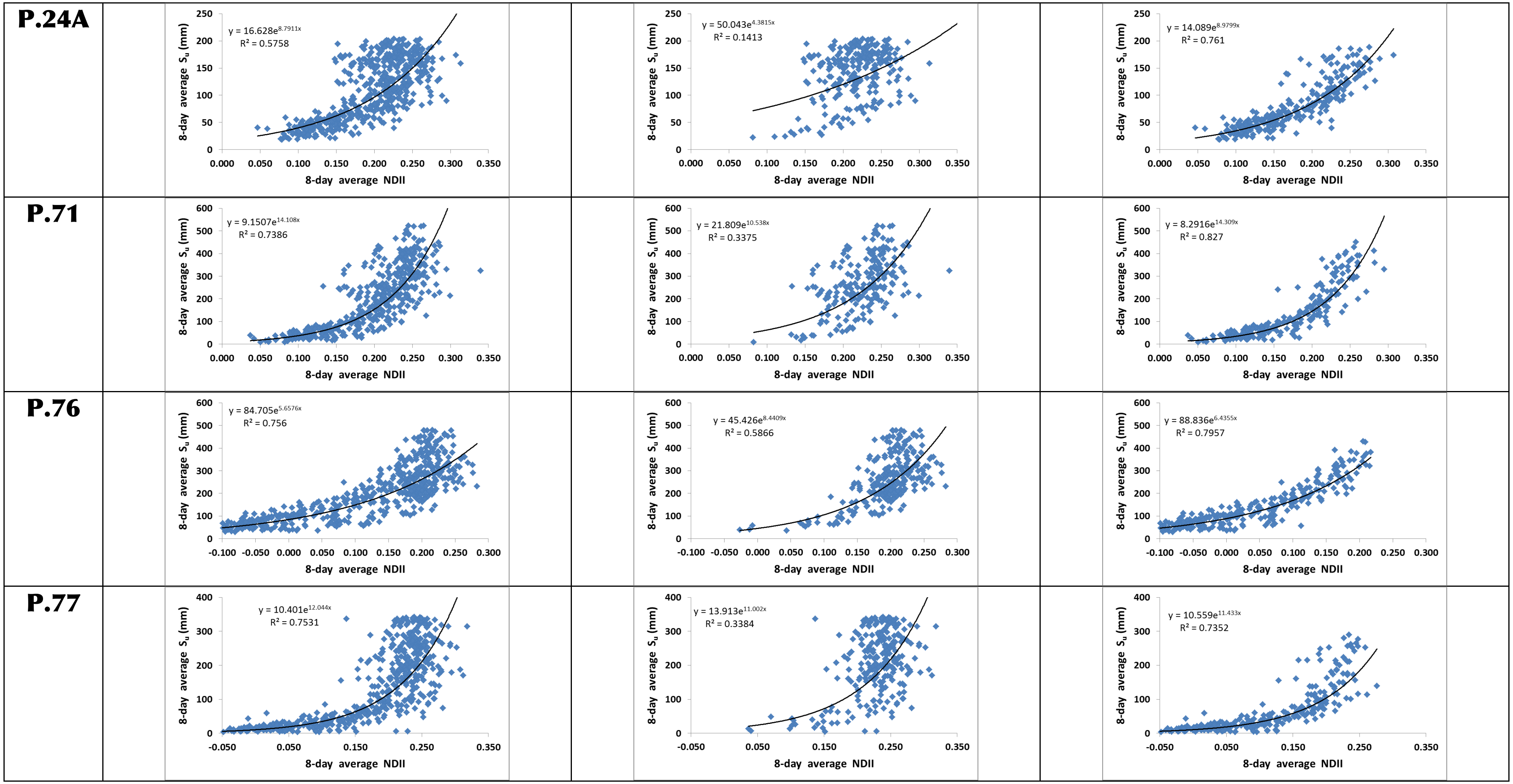

Figure 6. Scatter plots between the average NDII and the average root zone moisture storage (S_u) for 8 sub-basins controlled by runoff stations. Regression lines are added merely to illustrate the degree of correlation.

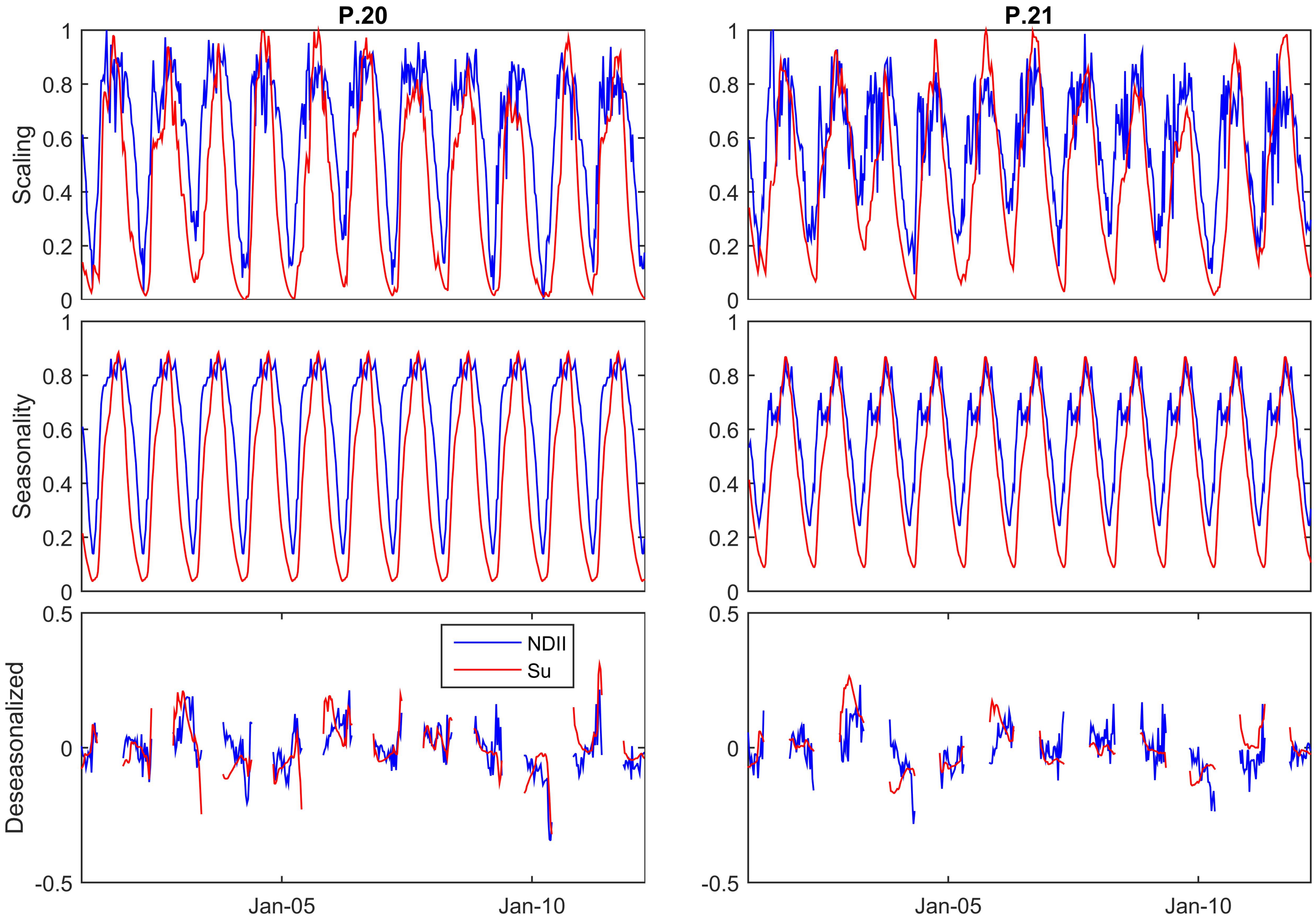

Figure 7. Scaled time series, seasonality and de-seasonalized (dry seasons) time series of the 8-days-averaged NDII values compared to the 8-days-averaged simulated root zone moisture storage (S_u) in Nam Mae Rim sub-basin at P.20 (Chiang Dao) and P.21 (Ban Rim Tai) runoff stations. The coefficients of determination (R^2) of the de-seasonalized NDII and S_u are 0.32 and 0.18 respectively for P.20 and P.21. For the results of all the 8 sub-basins, please refer to the supplementary material.